Analytical and Experimental Validation of Electromagnetic Simulations Using COMSOL®, re Inductance, Induction Heating and Magnetic Fields

Mark W. Kennedy[1], Shahid Akhtar[1], Jon Arne Bakken[1] and Ragnhild E. Aune[1,2]
[1]Dept. of Materials Science and Engineering, Norwegian University of Science and Technology (NTNU),
N-7491 Trondheim, NORWAY
[2]Dept. of Materials Science and Engineering, Royal Institute of Technology (KTH),
S-100 44 Stockholm, SWEDEN

Communicating author: mark.kennedy@ntnu.material.no

Abstract: COMSOL® is a powerful numerical modelling tool for electromagnetic calculations. The present paper examines the numerical agreement between COMSOL® 2D axial symmetric models, classical analytical solutions and experimental data. Comparison is made between the analytical solution for the inductance of an empty 'current sheet' inductor and the numerical results of COMSOL® Version 4.2, as a benchmark of the fundamental accuracy of the software. The effect of the size of the computational space or 'magnetic domain' on the calculated total inductance is also examined.

COMSOL®'s single and multi-turn domains are used to model an induction coil, and the simulations of induction heating are made at a range of frequencies from 50 Hz to 500 kHz. Results are compared with the predictions of a 1D analytical model at each frequency and a representative experimental value at 50 Hz. The obtained COMSOL® predictions of the magnetic flux density are compared with experimental values measured using Hall probes at 50 Hz, for both an empty coil and for a coil containing a work piece. The numerical magnetic field results obtained in the present study are in excellent agreement with the analytical solution for the 'air core' coil.

Based on the present results analytical criteria are presented as guidelines for when to use COMSOL®'s single or multi-turn domains, and for the minimum mesh size to be used to achieve accurate high frequency simulations of induction processes.

Keywords: Induction, inductance, heating, magnetic field.

1. Introduction

Re-heating of aluminium billets before forging or extrusion is a common application of induction heating technology. The process is driven by the magnetic flux created by a time varying current flowing in the induction coil, i.e. the magneto-motive force.

Coils used for induction heating are generally very short, and the magnetic fields which they produce are much weaker than what would be expected from the following equation for a long coil (the mathematical terms used in this paper are listed in Appendix 1: Table 1):

$$\left|\overrightarrow{B_\infty}\right| = \frac{\mu_o \mu_r N_c I_c}{l_c} \qquad (1)$$

The magnetic field on the centre line of a short coil can; however, be found by solving the Biot-Savart law, as presented in Figure 1 for 'air core' coils [1]:

$$\partial \vec{B} = \frac{\mu_o}{4\pi} \frac{I \vec{\partial l} \times \hat{r}}{r^2} \qquad (2)$$

In Figure (1) the integral of equation (2), B_o, is plotted as a ratio of B_∞ from Equation (1) versus a dimensionless coil length. Figure 1 indicates that to achieve the magnetic flux density predicted by Equation (1) anywhere in the coil, the coil must be extremely long, e.g. a length of 10 times its diameter. This is much longer than a typical induction coil, and it can therefore be concluded that induction coils are in general, 'short'.

Based on the results presented in Figure 1, the following observations are made which

counter some of the commonly accepted assumptions made regarding short coils:

1. A short coil does not have a homogeneous internal magnetic field in either the axial or radial direction (not indicated in Figure 1), or equivalently a negligible external magnetic field.
2. The magnetic flux density at either end of the coil is not half the value at the middle.
3. The magnetic flux density in the middle of the coil is not equal to that of an equivalent length of an infinite coil (i.e. one having the same number of turns per unit length).

In the present study the effect of the non-infinite nature of short coils will be examined by comparing inductance, induction and magnetic field strength estimated by various analytical equations, to experimentally measured data, as well as the numerical results of COMSOL®.

2. Governing Equations of the COMSOL® Model and Modelling Approach

In classical induction furnace theory the solutions are derived starting from the magnetic field intensity created by the coil [2]; however, they can also be derived beginning with the magnetic vector potential, $\vec{A}$, as given by Equation (3), and solved using the quasi-static approach ($\nabla \cdot \vec{J} = 0$) as presented in Equations (3)-(8) for zero velocity and ignoring the displacement current. Equations (8) and (9) are equivalent for sinusoidal currents:

$$\vec{B} = \nabla \times \vec{A} \tag{3}$$

$$\vec{B} = \mu_o \mu_r \vec{H} \tag{4}$$

$$\nabla \times \vec{H} = \vec{J} \tag{5}$$

$$\vec{J} = \sigma \vec{E} + \vec{J^e} \tag{6}$$

$$\vec{E} = \nabla V - \frac{\partial \vec{A}}{\partial t} \tag{7}$$

$$j\omega\sigma \vec{A_\phi} + \nabla \times \vec{H} = \vec{J^e} \tag{8}$$

$$\frac{\partial^2 \vec{A_\phi}}{\partial r^2} + \frac{1}{r}\frac{\partial A_\phi}{\partial r} + \frac{\partial^2 \vec{A_\phi}}{\partial z^2} - \frac{\vec{A_\phi}}{r^2} = \mu_o \mu_r \sigma \frac{\partial \vec{A_\phi}}{\partial t} \tag{9}$$

Considering the approximately cylindrical geometry of both the coil and the work piece, a cylindrical co-ordinate system was used in the present study, and the equations solved using 2D axial symmetric models. It should be noted that the errors obtained in estimating magnetic flux density introduced by modelling helical coils as a series of stacked loops, are generally very small (e.g. one part per thousand), and strongly depend on the spacing and angle of the coil turns [3]. All solutions reported have been calculated using current driven coils, which ensure that the correct magneto-motive force is present. The voltage and impedance in the coil domains may then be in error without causing any impact on estimated induction in the work piece.

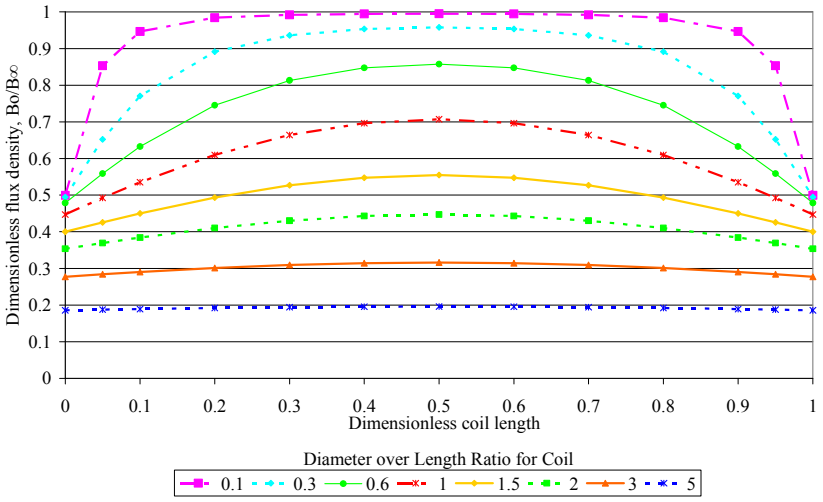

Figure 1. Dimensionless Flux Density (z-component) on the Centre Line of a Short 'Air core' Coil as a Function of Dimensionless Coil Length [1].

3. Inductance of a Short Coil

The inductance of a short coil, which is determined by the flux linkages per unit current, can be calculated using the method of Lorenz [4]. A more convenient method uses a tabulated correction factor, first published by Nagaoka [5] to six significant figures, which contains the solutions to the double elliptical integrals of Lorenz:

$$L_o = \frac{k_N A_c N_c \left|\overrightarrow{B_\infty}\right|}{I_c} \qquad (10)$$

For induction coils, k_N can also be estimated by the method of Knight [6] to approximately three significant figures:

$$k_N = \frac{1}{1 + 0.4502\left(\frac{D_c + \delta_c}{l_c}\right)} \qquad (11)$$

In the present study, the analytical solutions for k_N were estimated using numerical software available online, to more than 12 significant figures [7]. In evaluating k_N, the centre line of the round coil tubing was found to be the optimum reference diameter (least overall error), over the full range of frequencies from 50 Hz to 500 kHz.

As an example for inductance, an 'air core' 16 turn 'current sheet' coil is considered. This 'coil' was modelled using COMSOL® 4.2, and the results compared against the theoretical solution, i.e. Equation (10), in order to benchmark the accuracy of the COMSOL® software. A theoretical current sheet consists of one infinitely thin turn, with the current increased to $N_c I_c$ in order to represent the number of revolutions the current would make in a real helical coil. Using COMSOL®, the current sheet was modelled as a single 0.1 mm thick by 105.8 mm high copper sleeve, using the single-turn domain. The Nagaoka coefficient for this coil (k_N) is 0.639413 and from Equation (10), its inductance is 26.4051 μH. The measured value for a real tubular coil of the same overall dimensions was found to be 26.902 μH including lead effects.

The single turn inductance of the current sheet calculated by COMSOL® was adjusted to the value of the equivalent helical 16 turn coil, using the factor N_c^2 to account for the number of magnetic flux linkages and the true current per turn. Results were calculated as a function of the relative size of the 'magnetic domain' to the size of the coil. This was done in order to estimate the error introduced by the change of the external magnetic reluctance, on the flux density of the coil. The results obtained are presented in Table 1. More details of the models used in this paper can be found in Appendix 1: Table 2.

Table 1: Comparison between COMSOL® and Equation (10)

Ratio of Magnetic Domain Dimensions to Coil Dimensions	COMSOL Calculated Inductance (μH)	COMSOL - Analytical Solution Difference (%)
2.00	22.7563	-13.82
4.00	25.9502	-1.72
6.00	26.2783	-0.48
10.00	26.3870	-0.07
14.00	26.4057	0.00
20.00	26.4129	0.03

A ratio of 14, between the size of the coil and the size of the computational space, was selected as numerically sufficient to represent an infinite external volume with a negligible error in the coil's average internal magnetic flux density.

4. Induced Heating of a Cylindrical Work Piece

When circular eddy currents are induced in a work piece, heat is generated due to resistive heating by the portion of the current that is in phase with the voltage. The amount of heat generated is affected by the size and electrical conductivity of the work piece, the frequency and amount of the applied current, the number of turns in the coil, etc. The present authors have reviewed the classical approach for the computation of heat generation in a cylindrical work piece [2], and the equations can be summarized as follows:

$$P_w = k_N^{*2}\sqrt{2}\pi (I_c N_c)^2 \rho_w \xi_w \varphi(\xi_w)/l_c \qquad (12)$$

$$k_N^{*} = k_N\left(1 - \left(\frac{D_w - \delta_w}{D_c + \delta_c}\right)^2\right) + \left(\frac{D_w - \delta_w}{D_c + \delta_c}\right)^2 \qquad (13)$$

$$\xi_w = \frac{D_w}{\delta_w\sqrt{2}} \qquad (14)$$

$$\varphi(\xi_w) = \frac{\sqrt{2}(ber\xi_w ber'\xi_w + bei\xi_w bei'\xi_w)}{ber^2(\xi_w) + bei^2(\xi_w)} \qquad (15)$$

$$\delta_w = \left(\frac{\rho_w}{\pi\mu_r\mu_o f}\right)^{0.5} \qquad (16)$$

Equation (13) calculates the modified Nagaoka short coil correction factor first developed by Vaughan and Williamson [8] in 1945. This equation, which only accounts for the fraction of the volume of the coil occupied by the work piece and its effect on the magnetic flux density in the air-gap, is essential for obtaining accurate calculations for short coils. Appropriate frequency correction validated using COMSOL® has therefore been added to Vaughan and Williamson's original equation to account for the electromagnetic penetration into both the coil and the work piece. For tubular coils over the large range of frequencies examined in the present study, a good correlation was achieved by fixing the effective current sheet diameter to the average coil diameter in accordance with the classical approach for calculating coil inductance, i.e. $D_c+\delta_c = D_c$ measured at the tube centre-line.

Model simulations were performed using the input data summarized in Appendix 1: Table 2, for frequencies from 50 Hz to 500 kHz. The initial mesh (Mesh 1) is presented in Figure 2 (with the work piece indicated by a white outline). The heating results are summarized in Table 2 and compared to the values calculated using Equations (12) to (16).

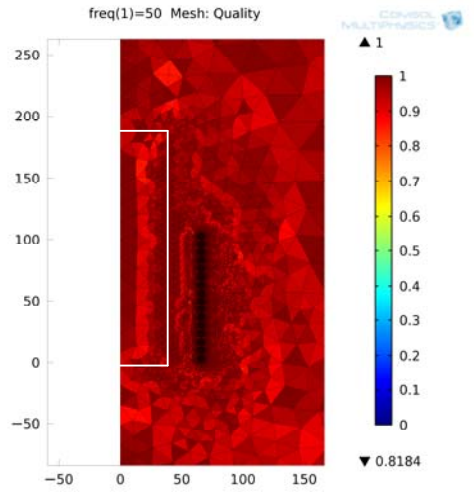

Figure 2. Mesh Quality for Mesh 1.

The electrical conductivity of the aluminium work piece was measured using an AutoSigma 3000 conductivity analyser (General Electric Inspection Technologies, UK) to within ±0.5%, calibrated against aluminium standards accurate to ±0.01% IACS. The electrical conductivity was not used as a fitting parameter. Actual power measurements were taken as described in detail elsewhere [2], using a Fluke 43B power quality analyser (Fluke, USA) and an i1000S inductive current probe (Fluke, USA), with a reproducibility of ~±6%. The resistive heating in the work piece at 50 Hz, for a coil excitation of 988.5 A, was determined to be 696 W, based on 2 readings.

Table 2: Comparison of Experimental, Analytical and COMSOL® Results for Mesh 1

Frequency (Hz)	Experimental Power (W)	Analytical Power (W)	Mesh 1 Power (W)	Mesh 1 - Analytical Difference (%)	δ (mm)
50	696	691	650	-6.0	14.50
500	N/A	2768	2604	-5.9	4.59
5000	N/A	9549	10280	7.7	1.45
50000	N/A	29697	24211	-18.5	0.46
500000	N/A	94123	25728	-72.7	0.14
	Mesh 1spacing at work piece interface =				5.10

The results presented in Table 2, clearly reveal that the accuracy of the COMSOL® results dramatically decreases as the mesh at the work piece/air-gap interface becomes coarser than the electromagnetic penetration depth; however, if the mesh is improved by the use of boundary elements, then accurate results can be obtained at very high frequency as presented in Table 3. It should be noted that with the electrical measuring technique presently used, it is not possible to determine if COMSOL® has any significant error in determination of the heat generation in the work piece. In future studies direct calorific measurements of the heat generation in the work piece will be performed.

Table 3: Comparison of Experimental, Analytical and COMSOL® Results for Mesh 2

Frequency (Hz)	Experimental Power (W)	Analytical Power (W)	Mesh 2 Power (W)	Mesh 2 - Analytical Difference (%)	δ (mm)
50	696	691	650	-6.0	14.5
500	N/A	2768	2597	-6.2	4.59
5000	N/A	9549	8834	-7.5	1.45
50000	N/A	29697	28305	-4.7	0.46
500000	N/A	94123	90029	-4.3	0.14
	Mesh 2 spacing at work piece interface =				0.02

It is possible to use the COMSOL® multi-turn domain with high frequency simulations of induction processes, but only if work piece data is the sole desired output. The work piece remains surrounded by the same magneto-motive force, and hence the induced power remains virtually constant (less than 1% change), regardless of frequency.

If information regarding the impedance of the coil is important, it is **essential to use the COMSOL® single-turn domain** when the

electromagnetic penetration depth into the coil is less than the thickness for a square conductor or the tube diameter for a circular conductor, i.e. if $\delta_c < t_c$.

If the electromagnetic penetration depth is smaller than the tube diameter, the current distribution will not be homogeneous over the volume of the tube. As the frequency increases the current will first be biased to the side of the conductors facing the coil centre line and subsequently be redistributed over the whole outer surface of the conductors, as presented in Figure 3. With a tubing diameter of 6 mm, a single-turn domain must be used above 168 Hz.

To use the COMSOL® single-turn domain, each turn must be modelled as a separate domain. Failure to do so will result in a non-physical vertical redistribution of the current as COMSOL® attempts to achieve the lowest possible coil impedance.

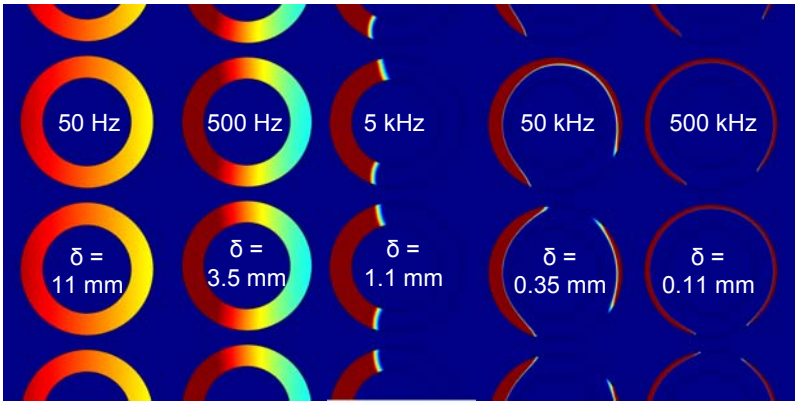

Figure 3. COMSOL® Results Showing Relative Current Distribution for Frequencies Ranging from 50 Hz to 500 kHz, (The Coil Centre Line is on the Left Side of the Conductors).

It is also necessary to insert boundary elements into the coil domains at high frequencies to accurately estimate: the current distribution, the inductance and most importantly the coil resistance. The same electromagnetic penetration depth criterion applies, i.e. the thickness of the boundary elements must be less than the electromagnetic penetration depth into the copper in the coil. Errors in estimating the coil resistance at high frequency using the multi-turn domain are given in Table 4.

Table 4: Comparison between Experimental, Analytical, Single and Multi-turn Estimates for Coil Resistance as a Function of Frequency

Frequency (Hz)	Experimental Coil Resistance (mΩ)	Mesh 2 Single-Turn Coil Resistance (mΩ)	Mesh 1 Single-Turn Coil Resistance (mΩ)	Multi-Turn Coil Resistance (mΩ)	Multi-Mesh 2 Single Difference (%)	δ (mm)
50	10.14	10.02	10.68	10.02	0.0	10.98
500	As above	10.56	13.26	10.02	-5.1	3.47
5000	25.70	24.57	33.91	10.02	-59.2	1.10
50000	91.40	81.78	97.90	10.02	-87.7	0.35
500000	300.30	289.89	325.50	10.02	-96.5	0.11
Yellow = analytical solution			Mesh 2 spacing at coil interface =			0.02

Based on the results presented in Table 4, it is clear that significant errors occur in the coil resistance estimates calculated using the multi-turn domain at frequencies for which the electromagnetic penetration depth is less than the coil tubing diameter, i.e. when the skin depth, coiling and proximity effects begin to have a major impact on the current distribution and therefore impedance [9-13].

5. Magnetic Field of an 'Air Core' Coil

A short 'air core' coil does not have a homogeneous magnetic field in either the axial or radial directions as explained in Section 1 and shown axially in Figure 1. Analytical solutions to determine the off-axis magnetic field strength of a coil do exist [14-17], but experimental values are reported in this study for physical validation. The direct measurements of the magnetic flux density of a real short coil in the present study were taken using a F.W. Bell model 6010 Gauss meter (Pacific Scientific OECO, USA). Standardized axial and radial Hall probes, with a measuring error of less than ±1% for AC magnetic fields were used. Accuracy was confirmed using axial standards of 0.05 and 0.2 T, and a transverse standard of 0.05 T, prior to use.

In Figure 4, axial experimental data for the air-core coil are plotted together with the

solution to Equation (2) for a coil diameter to length ratio of 1.24. The measurements were taken with a 6 mm diameter probe, and results plotted allowing for the average 3 mm off-set. As can be seen from Figure 4, there is excellent agreement between the experiment and analytical results, as well as the COMSOL® calculations. The small discrepancies near the coil wall are likely due to minor geometric imperfections in the stacking of the coil turns.

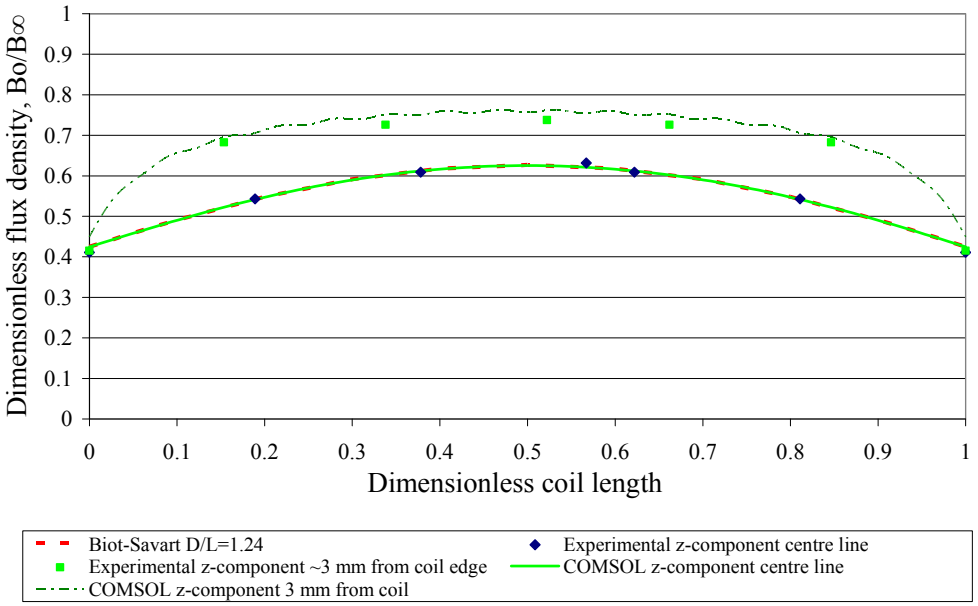

Figure 4. Dimensionless Magnetic Flux Density for a 16 Turn Induction Coil at 50 Hz, without a Work Piece.

6. Magnetic Field of a Coil Containing an A356 Aluminium Alloy Work Piece

The presence of the work piece will increase the magnetic flux density in the air gap of the coil as predicted by Equation (13), and indicated in Figure 5. The increase in the magnetic field strength is apparent by the difference between the Biot-Savart solution for an empty coil (dotted red line), the blue dots representing the measured values, and the green lines representing the COMSOL® calculated values 3 mm from the work piece and coil, respectively. The agreement between the actual measured and COMSOL® estimated values were typically ±1.5% with or without a work piece, except near the coil wall. Physical errors in the probe position (±0.5 mm), and the angle of alignment are the most likely source of discrepancies.

7. Conclusions and Future Work

Based on the present study the following conclusions and suggestions for future work are proposed:

- Comparison of the COMSOL® predictions against analytical models of known accuracy, proved critical in determining when the numerical model had achieved an acceptable level of precision.
- A magnetic domain 14 times as large as the dimensions of an induction coil is sufficiently large to accurately calculate the correct average magnetic flux density in the air-gap of the coil in the current model.
- Single-turn domains must be used if the frequency in the simulation is such that the electromagnetic penetration depth is less than the diameter of the coil tubing.
- Each turn of the coil must be modelled separately to prevent COMSOL® from redistributing the current in a non-physical manner.
- Meshing at the interface of both the work piece and the coil must be finer than the electromagnetic penetration depth in order to achieve accurate results when working at high frequencies.

- With proper experimental validation, meshing and selection of domains, it is believed that COMSOL® is capable of calculating electromagnetic phenomena as accurately as can be reasonably measured in the laboratory.
- Based on the accurate modelling of the power, i.e. induced current, as well as the magnetic flux density at the surface of the work piece, it is assumed that COMSOL® should predict electromagnetic Lorentz forces in the work piece with high accuracy.

The Lorentz forces and the resulting flow patterns developed in liquid aluminium will be explored in a future publication in relation to magneto-hydrodynamic modelling.

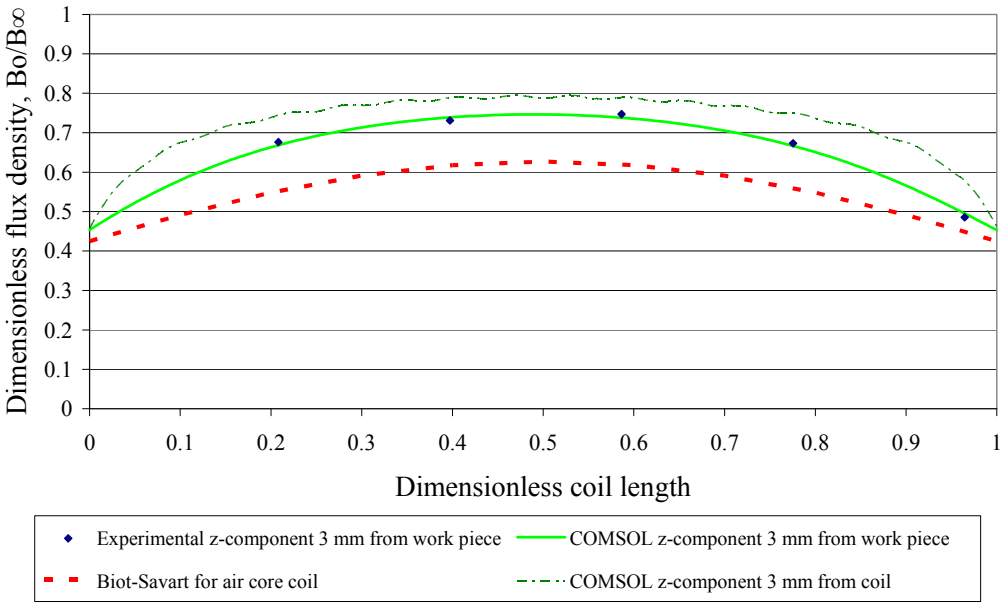

Figure 5. Dimensionless Magnetic Flux Density for a 16 Turn Induction Coil with 76.8 mm Diameter, with A356 Work Piece at 50 Hz.

8. Acknowledgements

This research was carried out as part of the Norwegian Research Council (NRC) funded BIP Project (No. 179947/I40) RIRA (Remelting and Inclusion Refining of Aluminium). The project partners are as follows: Hydro Aluminium AS, SAPA Heat Transfer AB, Alcoa Norway ANS, Norwegian University of Science and Technology (NTNU) and SINTEF Materials and Chemistry. Funding by the industrial partners and NRC is gratefully acknowledged.

The authors also wish to express their gratitude to Egil Torsetnes at NTNU, Trondheim, Norway, for helping with the design and construction of the experimental apparatus. Sincere gratitude is also due to Kurt Sandaunet at SINTEF, Trondheim, Norway, for his support and help, as well as for the use of the SINTEF laboratory.

9. Appendix 1

Table 1: Glossary of Units and Symbols

Quantity	Symbol	Scalar Quantity SI Unit	Abbr.
Magnetic potential (vector)	A	weber/meter	Wb/m
Area	A_c	meter^2	m^2
Magnetic flux density (vector)	B	tesla	T
Differential flux density (vector)	∂B	tesla	T
Differential length (vector)	$\partial \ell$	meter	m
Diameter	D	meter	m
Electric field (vector)	E	volt/meter	V/m
Frequency	f	hertz	Hz
Magnetic field (vector)	H	ampere/meter	A/m
Current, RMS	I	ampere	A
Current density (vector)	J	ampere/meter^2	A/m^2
Nagaoka short coil correction factor	k_N	unitless	-
Modified Nagaoka factor	k_N^*	unitless	-
Length	ℓ	meter	m
Inductance	L	henry	H
Turns	N	unitless	-
Resistive heating, RMS	P	watt	W
Radius	r	meter	m
Biot-Savart unit (vector)	$\hat{r}$	meter	m
Resistance	R	ohm	Ω
Tube diameter	t_c	meter	m
Time	t	seconds	s
Electric potential	V	volt	V
Electromagnetic penetration depth	δ	meter	m
Permeability of vacuum	μ_o	henry/meter	H/m
Relative permeability	μ_r	unitless	-
Dimensionless penetration depth	ξ	unitless	-
Electric conductivity	σ	siemens/meter	S/m
Electric resistivity	ρ	ohm meter	Ω m
Induction effectiveness factor	φ	unitless	-
Magnetic flux	Φ	weber	Wb
e	External		
o	Used for short coil form		
∞	Designates infinite coil form		
c	Coil		
w	Work piece		
ber	Kelvin function real part		
bei	Kelvin function imaginary part		
ber'	Derivative of ber		
bei'	Derivative of bei		

Table 2: Model Parameters

Model Parameter	Value	Unit
Work piece diameter	76.8	mm
Work piece height	192	mm
Work piece alloy	A356	-
Work piece conductivity	48%	IACS
Work piece conductivity	2.41E+07	S/m
Work piece temperature	54	C
Work piece relative magnetic permeability μ_r	1	-
Copper tubing diameter	6.0	mm
Copper tubing thickness	1.0	mm
Copper tubing conductivity	80%	IACS
Copper tubing conductivity	4.20E+07	S/m
Copper tubing temperature	43	C
Coil diameter average	131.5	mm
Coil height	105.8	mm
Coil current	988.5	A
Coil turns	16	-
Mesh 1 cells	12159	-
Mesh 1 quality	0.8184	Average
Mesh 2 cells	33713	-
Mesh 2 quality	0.7813	Average

10. References

1. M. W. Kennedy, S. Akhtar, J. A. Bakken, and R. E. Aune, "Electromagnetically Enhanced Filtration of Aluminum Melts," 2011 TMS Annual Meeting & Exhibition, Proceedings: Light Metals 2011 - Cast Shop for Aluminum Production, Ed. G. Brooks and J. Grandfield, San Diego, USA, February 27 - March 3, 2011.
2. M. W. Kennedy, S. Akhtar, J. A. Bakken, and R. E. Aune, "Review of Classical Design Methods as Applied to Aluminum Billet Heating with Induction Coils," 2011 TMS Annual Meeting & Exhibition, Proceedings EPD Congress 2011: Materials Processing Fundamentals, Ed. P. Anyalebechi and S. Bontha, San Diego, USA, February 27 - March 3, 2011.
3. C. Snow, "Formula for the inductance of a helix made with wire of any section," Ed: US Govt. Print. Off., 1926, p. 91.
4. L. Lorenz, "Ueber die Fortpflanzung der Electricität," *Annalen der Physik,* vol. 243, pp. 161-193, 1879.
5. H. Nagaoka, "The inductance coefficients of solenoids," *Journal of the College of Science,* vol. 27, pp. 18-33, 1909.
6. D. Knight, (2010, August 25), *3.1. Solenoids: Part 1.,* http://www.g3ynh.info [Online].
7. R. Weaver, (2011, July 26), http://electronbunker.sasktelwebsite.net/DL/NumericalExamples01.ods [Online]
8. J. Vaughan and J. Williamson, "Design of Induction-Heating Coils for Cylindrical Nonmagnetic Loads," *American Institute of Electrical Engineers, Transactions of the,* vol. 64, pp. 587-592, 1945.
9. R. Medhurst, "High Frequency Resistance and Self-Capacitance of Single-Layer Solenoids," *Wireless Engineer,* pp. 80-92, 1947.
10. E. Fraga, C. Prados, and D. Chen, "Practical model and calculation of AC resistance of long solenoids," *IEEE Transactions on Magnetics,* vol. 34, p. 205, 1998.
11. C. Hickman, "Alternating-Current Resistance and Inductance of Single Layer Coils," 1922.
12. S. Butterworth, "Eddy-current losses in cylindrical conductors, with special applications to the alternating current resistances of short coils," *Philosophical Transactions of the Royal Society of London. Series A, Containing Papers of a Mathematical or Physical Character,* vol. 222, pp. 57-100, 1922.
13. S. Butterworth, "Note on the Alternating Current Resistance of Single Layer Coils," *Physical Review,* vol. 23, pp. 752-755, 1924.
14. R. H. Jackson, "Off-axis expansion solution of Laplace's equation: Application to accurate and rapid calculation of coil magnetic fields," *Electron Devices, IEEE Transactions on,* vol. 46, pp. 1050-1062, 1999.
15. V. Labinac, N. Erceg, and D. Kotnik-Karuza, "Magnetic field of a cylindrical coil," *American journal of physics,* vol. 74, p. 621, 2006.
16. D. B. Montgomery and J. Terrell, Some useful information for the design of air-core solenoids: National Magnet Laboratory, Massachusetts Institute of Technology, 1961.
17. S. R. Muniz, M. Bhattacharya, and V. S. Bagnato, "Simple analysis of off-axis solenoid fields using the scalar magnetostatic potential: application to a Zeeman-slower for cold atoms," *Arxiv preprint arXiv:1003.3720,* 2010.